

1. Title: Effects of Equivalence Ratio Variations on Turbulent Flame Speed in Lean Methane/Air Mixtures under Lean-Burn Natural Gas Engine Operating Conditions

2. Authors: Zhiyan Wang¹, Emmanuel Motheau² and John Abraham^{1,2,3}

Affiliations:

¹School of Mechanical Engineering, Purdue University, West Lafayette, IN 47907

²School of Mechanical Engineering, University of Adelaide, South Australia 5005, Australia

³Department of Mechanical Engineering, San Diego State University, San Diego, CA 92182

3. Corresponding Author: Zhiyan Wang

Address:

School of Mechanical Engineering, Purdue University, West Lafayette, IN 47907, USA

Email: wang1695@purdue.edu

4. Colloquium: IC Engine Combustion

5. Total length of the paper: 5354 words (by Method 1)

6. Word equivalent length:

Main text: 2653 words

Equations: 114 words

References: 490 words

Tables(total): 851 words

Table 1: 291 words

Table 2: 277 words

Table 3: 283 words

Figures (total): 1246 words

Fig. 1: 123 + 20 = 143 words

Fig. 2: 248 + 15 = 263 words

Fig. 3: 129 + 21 = 150 words

Fig. 4: 165 + 34 = 199 words

Fig. 5: 129 + 36 = 165 words

Fig. 6: 128 + 37 = 165 words

Fig. 7: 128 + 33 = 161 words

7. N/A

Abstract

Direct numerical simulations (DNS) of turbulent premixed methane/air flames are carried out to investigate the effects of equivalence ratio on the turbulent flame speed in lean mixtures. Turbulent flames are simulated as statistically stationary following a Lagrangian framework using an inflow-outflow configuration. The inflow velocity is dynamically adjusted at run-time to stabilize the flame brush location within the computational domain. Linear forcing is applied inside the unburned mixtures to maintain the turbulent intensities at desired levels. For the same turbulence properties, several equivalence ratios near the lean limit are selected and it is shown that the normalized turbulent flame speed is a function of the equivalence ratio. Velocity and length scales of the imposed turbulence are then selected in such a way that the Karlovitz and Damköhler numbers remain constant for flames of different equivalence ratios. Simulations are run for more than 80 eddy turnover times and the turbulent flame speed is derived by averaging the inflow velocity. The results show that equivalence ratio does not have an explicit effect on the normalized turbulent flame speed above the lean limit. Examining the flame surface statistics, it is shown that the flame surface normal is preferentially parallel to the most compressive strain rate direction for all equivalence ratios.

Keywords

DNS of turbulent premixed flames, premixed flame speed, lean-burn, natural gas engines

1. Introduction

In recent years, natural gas has received increased attention as an alternative fuel source for internal combustion engines employed in transportation and power generation applications. It is known that natural gas produces 25-30% less carbon emissions per unit energy than conventional fuels [1, 2]. Lean burn natural gas engines are particularly attractive because of their potential of lower NO_x emissions and enhanced thermal efficiency compared to engines operating under stoichiometric conditions. However, lean burn also increases the likelihood of misfire due to combustion instabilities that result in increased exhaust emissions and reduced efficiency [3-5]. To address the challenges associated with lean burn, various strategies have been proposed including using elevated inlet manifold temperatures, hot-gas jet ignition and introducing greater swirl and turbulence at the end of compression [6]. The effectiveness of these approaches is often assessed with the aid of high-fidelity numerical tools.

Flamelet-based models are one of the most widely used models in modeling premixed turbulent combustion. For example, the G-equation model is based on the premise that the premixed turbulent flame could be represented by the isosurface of a scalar field G [7, 8]. The instantaneous flame front, assumed to be infinitely thin, is represented by an isosurface of the scalar quantity G at $G \equiv 0$. In the transport equation for G , turbulent flame speed S_T is used to model the global effects of turbulence on enhancing chemical reaction rates through flame surface augmentation and enhanced transport. The use of a single variable S_T greatly simplifies the modeling by eliminating the stiff chemistry source terms. Indeed, by assuming *á priori* closure for the turbulent flame speed, multi-dimensional simulations have been carried out in rather complex geometries such as bombs [9, 10], SI engines [11, 12] and industrial burners [13, 14].

It is important to note that several definitions of turbulent flame speeds exist. To avoid ambiguity, in this paper we will define turbulent flame speed as the velocity at which the unburned mixture enters the flame zone in the direction normal to the mean flame front. Numerous correlations for S_T has been proposed in the past and a majority of the existing correlations involves the ratio of velocity, i.e. u_{rms}/S_L , and that of the length scales, i.e. L_o/δ_L [13, 15-17]. Here, S_L and δ_L denote the flame speed and flame thickness of an unstrained laminar flame, respectively, while u_{rms} and L_o represents the root-mean-square of turbulent velocity fluctuations and the integral length scale, respectively.

The effects of equivalence ratio (ϕ) on S_T normalized by the laminar flame speed S_L are still not well understood. This understanding is of importance in lean-burn engines where fluctuations in equivalence ratios can be consequential on engine performance and where efficiency and emissions considerations require operation as close to the lean limit as possible. Specifically, it is not known whether the equivalence ratio effect is exerted only through its effect

on the laminar flame speed S_L . Limited work has been carried out to characterize the equivalence ratio effects. Bell *et al.* (2006) performed “2D” DNS of premixed methane flames at equivalence ratios $\phi = 0.55$ and 1.00 [18]. They found a change in the Markstein number as ϕ is varied which, in turn, modified the turbulent flame speed. Fru *et al.* (2011) carried out DNS of premixed methane-air flame kernels subjected to various turbulence intensities at five equivalence ratios [19]. They observed that for a fixed value of u_{rms}/S_L , S_T/S_L varies with equivalence ratios. However, neither of the two works has taken into account the effects of length scales, i.e. L_o/δ_L . In addition, the studied flames are subjected to decaying turbulence which introduces ambiguity into the definition of u_{rms}/S_L .

In this work, we set out to investigate the influence of equivalence ratio on the turbulent flame speed using DNS. By forcing the turbulence inside the fresh mixtures, we ensure that the premixed flame is interacting with non-decaying turbulence such that velocity and length scale ratios between the flow field and flame are clearly defined and held invariant. The rest of the paper is organized in the following manner. Section 2 will discuss the numerical methods, chemistry mechanism and the simulation setup. Section 3 presents the results of turbulent flame speed at various equivalence ratios. The effects of flow strain rates with respect to the flamelet are also discussed. The paper then closes with summary and conclusions in Section 4.

2. Computational Setup

2.1 The Numerical Model

The results presented in this work are obtained using the in-house low-Mach code HOLOMAC (High-Order LOW-MACH number Combustion) [20]. It solves the 3D conservation equations for multi-component mixtures with CHEMKIN interface for computing the chemical source terms. Spatial discretization is performed using a 6th-order implicit compact scheme [21].

The convection terms are advanced in time using a 2nd-order Adams-Bashforth (AB2) scheme while the diffusion terms are advanced using an explicit 4-step Runge-Kutta-Chebyshev (RKC) method. The divergence condition is enforced using a projection-correction method, i.e. at each time step, the hydrodynamic pressure is solved from a variable-coefficient Poisson equation using Fast Fourier Transform (FFT) and is used to correct the provisory velocity.

It is well known that DNS with multi-step chemistry is computationally intensive. In this work, a global chemical mechanism has been employed with the form shown in Eq. (1) that is able to predict the laminar flame speed:

$$\dot{\omega} = AT^b[\text{CH}_4]^m[\text{O}_2]^n e^{-E_a/RT}. \quad (1)$$

The parameters A , b , m and n are calibrated such that the laminar flame speed is comparable to the flame speed predicted by both a 17-species, 73-step skeletal mechanism developed by Sankaran *et al.* (2007) and the GRI-Mech 3.0 [22, 23]. Figure 1 shows the computed laminar flame speeds obtained with the three mechanisms for premixed equivalence ratios between 0.39 and 0.60, the range of interest in these simulations. The results agree within 2% of each other.

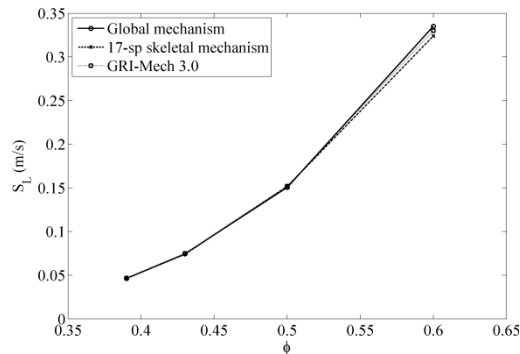


Fig. 1. Computed laminar flame speed as a function of ϕ for unburned temperature of 810 K at pressure of 20 bar.

2.2 Modeling of Statistically Stationary Flames

The turbulent premixed flame is simulated as statistically stationary inside the computational domain by employing a Lagrangian framework, i.e. the frame of reference is placed on the mean flame front and the cold premixed flow is "seen" as propagating toward a locally-

evolving but globally-stationary flame. This can be realized using an inflow-outflow configuration as shown in Fig. 2. Periodic boundary conditions are applied to the lateral boundaries parallel to the mean flow direction. Inflow of unburned methane-air mixture is specified at the left boundary while the burned flow passes through a sponge zone and exits from the right. To maintain the flame stationary, *á priori* knowledge of the flame speed is required to specify the inflow boundary condition. This information is, however, not readily available and is the interest of the simulation. Instead, a predictive control is employed on the mean flame position to correct the bulk inflow velocity toward the "true" flame speed. In the current simulations, two forms of control loop have been implemented. A differential loop is used to adjust inflow velocity until the mean flame front is stationary within a characteristic time period τ_d . In addition, an integral control is applied to return the mean flame front to its initial position over some characteristic time τ_i . To minimize interference between the two forms of feedback control, the characteristic time scale of the integral control τ_i has been selected to be much longer than τ_d .

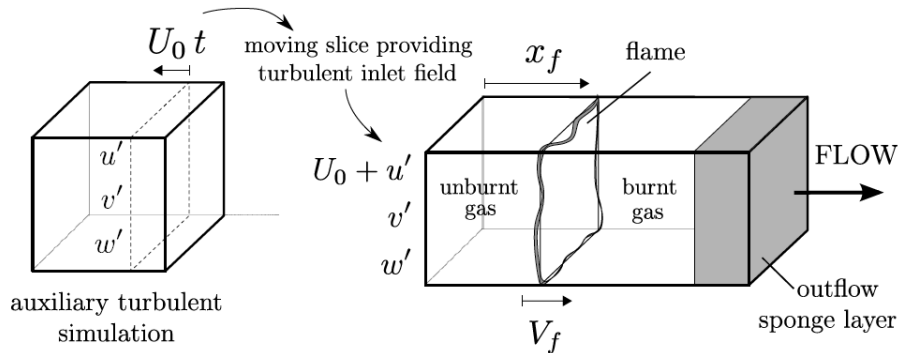


Fig. 2. Schematic of the inflow-outflow configuration for simulation of the turbulent premixed flame as statistically stationary.

The domain is initialized with a laminar flame. To maintain the desired turbulence intensity in the reactants, turbulent fluctuations are imposed on the bulk inflow velocity. These fluctuations are obtained from the moving slice of a homogeneous isotropic turbulent field generated in an

auxiliary simulation. In addition, the unreacted flow ahead of the flame is forced using a "linear forcing" scheme of the form [24]:

$$F_i = M(T)B \left[\frac{k_o}{k} \right] u_i. \quad (2)$$

This term is added to right-hand-side of the momentum equation to represent the energy cascade from scales which are larger than the domain size. Here, k is the instantaneous turbulent kinetic energy (TKE) in the reactant mixture and k_o is the desired steady-state TKE. $M(T)$ is a ramp function of temperature which decreases from 1 to 0 as T increases by 200 K above the unburned temperature. This is to prevent any artificial effect of forced turbulence on the flame structure. B is the forcing constant which is inversely proportional to the steady-state eddy turnover time. It has been reported that the integral length scale, L_o , of the forced turbulence will always converge to approximately 20% of the domain size independent of its initial state or the choice of the forcing constant B [25]. This means that L_o can be fixed by selecting an appropriate domain size and consequently a constant ratio of L_o/δ_L can be maintained throughout the simulation. Figure 3 shows the time-averaged turbulent kinetic energy spectrum in the wavenumber space for a homogeneous isotropic turbulence of a turbulent Reynolds number $Re_T = 880$ generated by "linear forcing".

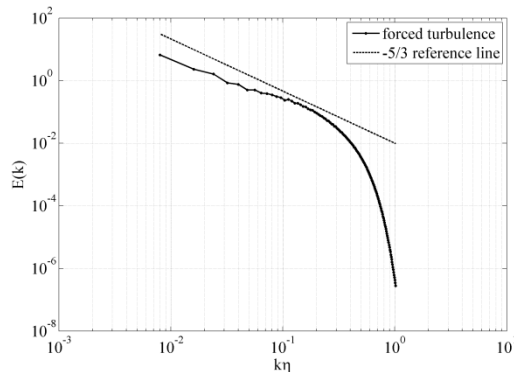


Fig. 3. Spectrum of turbulent kinetic energy as a function of wavenumber normalized with the Kolmogorov scale for turbulence sustained by linear forcing.

3. Results and Discussion

We will now present results from the parametric studies exploring the effects of equivalence ratio on turbulent flame speed under lean-burn conditions. Each simulation is performed over more than 80 eddy turnover times to obtain a large sample space for meaningful statistics to be collected. Pressure is selected at 20 bar and the reactant temperature at 810 K, reflective of engine conditions. The equivalence ratio is varied from 0.39 to 0.5 while the turbulence properties are kept constant as shown in Table 1.

Table 1

Computational parameters and turbulence conditions employed in this study. Computed normalized turbulent flame speeds are also listed.

| | Case 1 | Case 2 | Case 3 |
|-----------------------------------|-------------|-------------|-------------|
| Domain size (mm ³) | 8.0×3.2×3.2 | 8.0×3.2×3.2 | 8.0×3.2×3.2 |
| ϕ | 0.50 | 0.43 | 0.39 |
| S_L (m/s) | 0.1506 | 0.07445 | 0.04650 |
| δ_L (μm) | 100 | 200 | 300 |
| u_{rms} (m/s) | 2.160 | 2.160 | 2.160 |
| L_o (mm) | 0.64 | 0.64 | 0.64 |
| u_{rms}/S_L | 14.34 | 29.01 | 46.45 |
| L_o/δ_L | 6.40 | 3.20 | 2.13 |
| Re_T | 315 | 315 | 315 |
| Da | 0.45 | 0.11 | 0.05 |
| Ka | 21.5 | 87.4 | 216.8 |
| S_T/S_L | 10.2±1.3 | 7.9 | 7.1 |

The turbulent flame speed S_T can be obtained from the time average of the bulk inflow velocity once the turbulent flame becomes fully-developed and stationary in the statistical sense. Table 1 shows the statistically stationary turbulent flame speed S_T normalized by S_L for the various cases. It can be seen that as equivalence ratio is reduced from 0.5 to 0.43 and 0.39, S_T/S_L decreases from 10.2 to 7.9 and 7.1, respectively. This is possibly because the leaner flames are more susceptible to extinction when subjected to the same level of turbulence, thereby reducing the flame surface area and consequently S_T/S_L . This would suggest that equivalence ratio has an effect on the turbulent flame speed. At this point, the question arises as to whether this effect of equivalence ratio can be modeled through other parameters which may be influencing the speed. Note that when equivalence ratio is changed, the chemical timescales change with respect to the turbulence timescales. Two parameters that account for this change in timescales are the Karlovitz number (Ka) and Damköhler number (Da). The Karlovitz number represents the ratio of characteristic chemical timescale to the Kolmogorov timescale while Damköhler number represents the ratio of integral eddy turnover time to the chemical timescale. Their respective definitions used in this paper are given as,

$$Ka = \frac{\tau_c}{\tau_\eta} \sim \left(\frac{u_{rms}}{S_L} \right)^{\frac{3}{2}} \left(\frac{\delta_L}{L_o} \right)^{\frac{1}{2}}, \quad (3)$$

$$Da = \frac{\tau_t}{\tau_c} \sim \frac{S_L}{u_{rms}} \frac{L_o}{\delta_L}. \quad (4)$$

To understand if these parameters, rather than equivalence ratio, can account for the change in the normalized turbulent flame speeds, the equivalence ratio is varied while the turbulence properties are also varied to keep the non-dimensional turbulence intensity, Da and Ka to be constant. Table 2 lists the physical conditions employed for these simulations. The pressure is set at 20 bar and unburned mixture temperature at 810 K as before. Turbulent velocity fluctuations

are varied between 0.67 - 4.81 m/s such that u_{rms}/S_L remains constant at 14.3. The computational domain size is selected at $80 \times 32 \times 32\delta_L$ such that L_o is always 6.4 times the laminar flame thickness. Figure 4 shows volume rendering of the flames when the equivalence ratios are changed from 0.39 to 0.60 but the non-dimensional turbulence intensity, Da and Ka are unchanged. There is no visual difference in the extent of wrinkling of the flame surface at these two equivalence ratios despite the fact that the turbulence intensity in Fig. 4(b) is 7.2 times greater than that in Fig. 4(a).

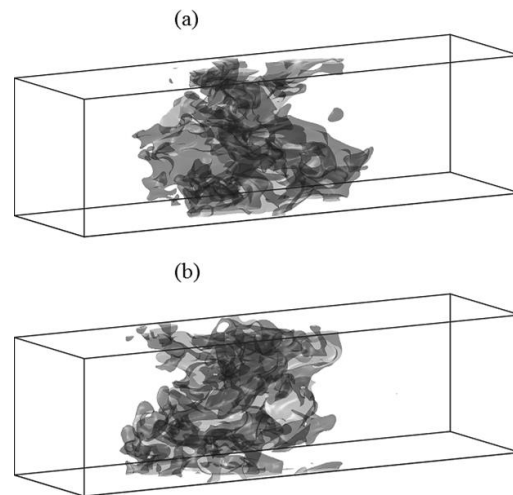


Fig. 4. Volume rendering of temperature isosurface of $T = 1400$ K for DNS of flames of (a) $\phi = 0.39$ (Case 3a) and (b) $\phi = 0.60$ (Case 4) with constant u_{rms}/S_L , Da and Ka .

Table 2

Computational parameters and turbulence conditions which keep Da and Ka constant. Computed normalized turbulent flame speeds are also listed.

| | Case 1 | Case 2a | Case 3a | Case 4 |
|-----------------------------------|-------------|--------------|--------------|-------------|
| Domain size (mm ³) | 8.0×3.2×3.2 | 16.0×6.4×6.4 | 24.0×9.6×9.6 | 4.0×1.6×1.6 |
| ϕ | 0.50 | 0.43 | 0.39 | 0.60 |
| S_L (m/s) | 0.1506 | 0.07445 | 0.04650 | 0.3351 |
| δ_L (μm) | 100 | 200 | 300 | 50 |
| u_{rms} (m/s) | 2.160 | 1.068 | 0.667 | 4.806 |
| L_o (mm) | 0.64 | 1.28 | 1.92 | 0.32 |
| u_{rms}/S_L | 14.34 | 14.34 | 14.34 | 14.34 |
| L_o/δ_L | 6.40 | 6.40 | 6.40 | 6.40 |
| Da | 0.45 | 0.45 | 0.45 | 0.45 |
| Ka | 21.5 | 21.5 | 21.5 | 21.5 |
| S_T/S_L | 10.2±1.3 | 10.2±1.2 | 9.9±1.2 | 10.4±1.0 |

Table 2 lists the normalized turbulent flame speeds and the standard deviations for the various cases. Interestingly, the normalized turbulent flame speed S_T/S_L has a similar value around 10 (within 5%) when u_{rms}/S_L , Da and Ka are unchanged. This suggests that the primary effect of equivalence ratio on turbulent flame speed is through its influence on the laminar flame speed S_L and the Ka and/or Da . Changing ϕ while holding the turbulence intensity constant (Case 1, 2 and 3 of Table 1) affects the ratios of velocities and length scales between the turbulence and the flame, i.e. u_{rms}/S_L and L_o/δ_L and consequently affects the flame speed S_T .

To confirm the validity of this result, simulations are carried out with a lower normalized turbulence intensity ($u_{rms}/S_L = 8.0$) for equivalence ratio of 0.5, 0.43 and 0.39. The integral length scale is again selected as 6.4 times the laminar flame thickness, and consequently Da and Ka are kept constant at 0.80 and 8.9, respectively. Pressure and unburned mixture temperature are selected to be 20 bar and 810 K, respectively. Table 3 lists the physical conditions employed for these simulations. The normalized turbulent flame speeds S_T/S_L are also tabulated with their standard deviations in Table 3. It is found that S_T/S_L is again approximately constant (around 8.6) when ϕ is changed but holding u_{rms}/S_L , Da and Ka invariant.

Table 3

Computational parameters for cases with a lower normalized turbulence intensity which keep Da and Ka constant. Computed normalized turbulent flame speeds are also listed.

| | Case 5 | Case 6 | Case 7 |
|-----------------------------------|-------------|--------------|--------------|
| Domain size (mm ³) | 8.0×3.2×3.2 | 16.0×6.4×6.4 | 24.0×9.6×9.6 |
| ϕ | 0.50 | 0.43 | 0.39 |
| S_L (m/s) | 0.1506 | 0.07445 | 0.04650 |
| δ_L (μm) | 100 | 200 | 300 |
| u_{rms} (m/s) | 1.205 | 0.596 | 0.372 |
| L_o (mm) | 0.64 | 1.28 | 1.92 |
| u_{rms}/S_L | 8.0 | 8.0 | 8.0 |
| L_o/δ_L | 6.40 | 6.40 | 6.40 |
| Da | 0.80 | 0.80 | 0.80 |
| Ka | 8.9 | 8.9 | 8.9 |
| S_T/S_L | 8.9±0.8 | 8.4±0.7 | 8.6±0.9 |

It is also interesting to investigate the statistics of the alignment of principal strain rate directions when equivalence ratio is changed. This provides insights on whether passive scalar gradients are created or destroyed by turbulence [26]. The principal strain rates are computed from the strain rate tensor S_{ij} at three different isotherm surface by solving the eigenvalues. The largest eigenvalue, denoted as λ_1 is called the most extensive strain rate and the smallest eigenvalue λ_3 is called the most compressive strain rate. Figure 5 shows the probability density function (pdf) of the orientation (expressed as cosine of the angle) between the principal strain rate directions and the local flame surface normal on the temperature isosurface at $T = 1694, 1394$ and 1094 K. Here, 1694 K corresponds to the temperature where heat release rate is maximum and 1094 K corresponds to the preheat zone of the flame of $\phi = 0.43$. It is shown that the most compressive strain rate direction is preferentially aligned to the flame surface normal while the most extensive strain rate direction is preferentially perpendicular to it. This suggests that the flame is strained in such a way that the isosurface of temperature (and also species mass fractions) are packed closer together and thereby facilitate steeper scalar gradients. Furthermore, the alignments do not show noticeable difference at various points across the flame. Comparison of the alignment in the preheat zone of flames at different equivalence ratios are illustrated in Fig. 6. The isotherm contour where data is analyzed is at 30% of the maximum temperature rise. Similar trend is observed for all four cases. This suggests that ϕ has limited explicit influence on turbulence-flame alignment in lean premixed flames suggesting that the fundamental turbulent flame structure is not altered. Figure 7 shows the pdf of the alignment between the principal strain rates and flame surface normal for $\phi = 0.5$ at an isosurface of $T = 1220$ K for $u_{rms}/S_L = 14.3$ and 8.0 (Case 1 and Case 5). The alignments between the most compressive strain rate and the flamelet normal show no visual difference when turbulence intensity is changed.

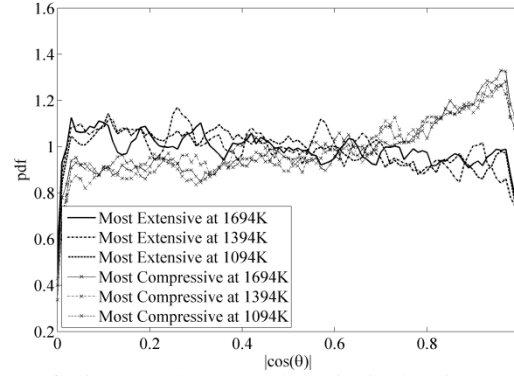


Fig. 5. Probability density function of alignment between the principal strain rate directions and flamelet normal on the isosurface of $T = 1694\text{K}$, 1394K and 1094K for $\phi = 0.43$ and $u_{\text{rms}}/S_L = 14.3$ (Case 2a).

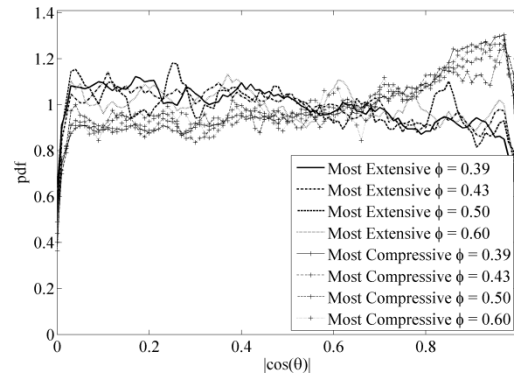


Fig. 6. Probability density function of alignment between the principal strain rate directions and flamelet normal in the flame preheat zone for $\phi = 0.39, 0.43, 0.50$ and 0.60 and $u_{\text{rms}}/S_L = 14.3$ (Case 1, 2a, 3a and 4).

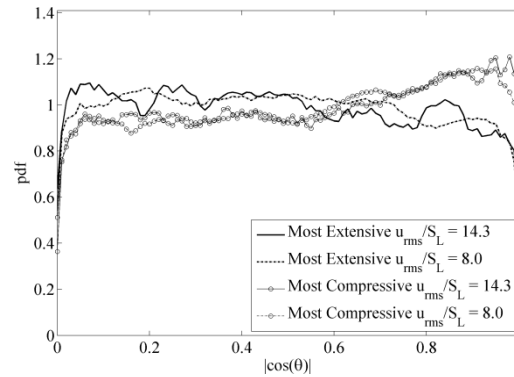


Fig. 7. Probability density function of alignment between the principal strain rate directions and flamelet normal in the flame preheat zone for $\phi = 0.50$ and $u_{\text{rms}}/S_L = 14.3$ and 8.0 (Case 1 and 5).

4. Summary and Conclusions

Direct numerical simulations of turbulent premixed methane flames are carried out under lean conditions using an inflow-outflow configuration. The flames are simulated as statistically stationary by dynamically adjusting the bulk inflow velocity. It is found that the normalized

turbulent flame speed, i.e. S_T/S_L , does not change with equivalence ratio above the lean limit when Ka and Da are fixed. This implies that ϕ only influences S_T implicitly by affecting ratios of length scales and velocities between turbulent flow and the flame. It is also found that the most compressive strain rate in the flow is preferentially aligned to the flame surface normal whereas the most extensive strain rate is preferentially perpendicular to it. In this way, steeper passive scalar gradients are generated by turbulence. Varying equivalence ratio does not influence turbulence-flame alignment.

Acknowledgements

The authors thank Caterpillar, Inc. for their financial support of this work. This work used the Extreme Science and Engineering Discovery Environment (XSEDE) which is supported by National Science Foundation grant number ACI-1053575, and computational resources provided by Information Technology at Purdue (ITaP).

References

- [1] K. Kato, K. Saeki, H. Nishide, T. Yamada, *JSAE Rev.* 22 (2001), 365-368.
- [2] R. Tilagone, G. Monnier, A. Chaouche, Y. Baguelin, S. De Chauveron, *SAE Technical Paper* 961080 (1996).
- [3] A. Das, H.C. Watson, *Proc. Inst. Mech. Eng.* 211 (1997) 361-378.
- [4] K.S. Varde, G.M.M. Asar, *SAE Technical Paper* 2001-28-0023.
- [5] M.L. Franklin, D.B. Kittelson, R.H. Leuer, M.J. Piphro, *SAE Technical Paper* 940546 (1994).
- [6] H.M. Cho, B.Q. He, *Energy Convers. Mgmt.* 48 (2007) 608-618.
- [7] F.A. Williams, *Combustion Theory*, Westview Press, Boulder CO, 1985.
- [8] J. Abraham, F.A. Williams, F.V. Bracco, *SAE Technical Paper* 850345 (1985).
- [9] B. Lewis, G. von Elbe, *Combustion, flames and explosions of gases*, Academic Press, New York, 1961.
- [10] T.W. Lee, G.L. North, D.A. Santavicca, *Combust. Sci. Tech.* 84 (1992) 121-132.
- [11] Y. D'Angelo, G. Joulin, G. Boury, *Combust. Theory Model* 4 (2000) 317-338.
- [12] R.N. Paul, K.N.C. Bray, *Proc. Combust. Inst.* 26 (1996) 259-266.
- [13] V. Zimont, W. Polifke, M. Bettelini, W. Weisenstein, *J. Eng. Gas Turbines Power* 120 (3) (1998) 526-532.
- [14] P. Flohr, H. Pitsch, *Proc. CTR Summer Program* (2000) 169-179.
- [15] P. Clavin, F.A. Williams, *J. Fluid Mech.* 116 (1982) 251-282.
- [16] A.R. Kerstein, *Proc. Combust. Inst.* 21 (1988) 1281-1289.

- [17] S. Daniele, P. Jansohn, J. Mantzaras, K. Boulouchos, Proc. Combust. Inst. 33 (2011) 2937-2944.
- [18] M.S. Day, J.B. Bell, J.F. Grcar, M.J. Lijewski, Proc. ECCOMAS-CFD (2006).
- [19] G. Fru, D. Thevenin, G. Janiga, Energies 4 (2011) 878-893.
- [20] E. Motheau, J. Abraham, J. Comp. Phys. under review.
- [21] S.K. Lele, J. Comp. Phys. 103(1) (1992) 16-42.
- [22] R. Sankaran, E.R. Hawkes, J.H. Chen, T.F. Lu, C.K. Law, Proc. Combust. Inst. 31 (2007) 1291-1298.
- [23] G.P. Smith, D.M. Golden, M. Frenklach, N.W. Moriarty, B. Eiteneer, M. Goldenberg, C.T. Bowman, R.K. Hanson, S. Song, W.C. Gardiner, Jr., V.V. Lissianski, Z. Qin, available at <http://www.me.berkeley.edu/gri_mech/> .
- [24] P.L. Carroll, G. Blanquart, Phys. Fluid 25 105114 (2013).
- [25] C. Rosales, C. Meneveau, Phys. Fluid 17 095106 (2005).
- [26] N. Chakraborty, N. Swaminathan, Phys. Fluid 19 (2007).

List of Figure Captions

Fig. 1. Computed laminar flame speed as a function of ϕ for unburned temperature of 810 K at pressure of 20 bar.

Fig. 2. Schematic of the inflow-outflow configuration for simulation of the turbulent premixed flame as statistically stationary.

Fig. 3. Spectrum of turbulent kinetic energy as a function of wavenumber normalized with the Kolmogorov scale for turbulence sustained by linear forcing.

Fig. 4. Volume rendering of temperature isosurface of $T = 1400$ K for DNS of flames of (a) $\phi = 0.39$ (Case 3a) and (b) $\phi = 0.60$ (Case 4) with constant u_{rms}/S_L , Da and Ka .

Fig. 5. Probability density function of alignment between the principal strain rate directions and flamelet normal on the isosurface of $T = 1694$ K, 1394 K and 1094 K for $\phi = 0.43$ and $u_{rms}/S_L = 14.3$ (Case 2a).

Fig. 6. Probability density function of alignment between the principal strain rate directions and flamelet normal in the flame preheat zone for $\phi = 0.39, 0.43, 0.50$ and 0.60 and $u_{rms}/S_L = 14.3$ (Case 1, 2a, 3a and 4).

Fig. 7. Probability density function of alignment between the principal strain rate directions and flamelet normal in the flame preheat zone for $\phi = 0.50$ and $u_{rms}/S_L = 14.3$ and 8.0 (Case 1 and 5).